and the observation of many more level spacings are expected to lead to a better understanding of the level spacings.

It has been pointed out by Sailor[27] that for s-wave neutron resonances the compound nucleus appears to be formed preferentially by the spin state $J=I+\frac{1}{2}$ rather than by an even distribution between the states $J=I+\frac{1}{2}$ and $I-\frac{1}{2}$. The present results tend to agree with this observation. Five of the seven s-wave resonances were assigned to the spin state $J=I+\frac{1}{2}$ and the level at -23 kev appears to be an s-wave level having this same value of the spin.

Finally, it was found after offering an explanation for the low cross section in the region below 30 kev that the potential scattering cross section of this nucleus is very closely given by the expression

$$\sigma_p=\sum_l(2l+1)4\pi\lambda^2\sin^2\delta_l,$$

and one could have proceeded just as well with the analyses by tacitly assuming this value of the potential scattering cross section.

[27] V. L. Sailor, Phys. Rev. **104**, 736 (1956).

ACKNOWLEDGMENTS

In conclusion, I wish to express my appreciation to Dr. L. A. Turner for his suggestions and criticisms, to Dr. F. E. Throw for his comments and suggestions with the manuscript, to Dr. Norbert Rosenzweig and Dr. J. E. Monahan for their discussions concerning the distributions of the angular momenta, the level spacings and the neutron widths, to Dr. J. P. Schiffer for his discussions concerning the strength functions and size distribution of the neutron widths, to Jack Wallace for his aid in operating the Van de Graaff generator, and to the Van de Graaff crew consisting of Walter Ray, Jr., William Evans, Ronald Amrein, Robert Kickert, John Bicek, Edward Saller, and Robert Petersen.

PHYSICAL REVIEW VOLUME 114, NUMBER 1 APRIL 1, 1959

Differential Elastic Scattering of Neutrons from Neon

H. O. COHN AND J. L. FOWLER
Oak Ridge National Laboratory, Oak Ridge, Tennessee
(Received November 12, 1958)

Neutron elastic scattering from neon of natural abundance has been investigated in the energy range 0.8 to 1.9 Mev. The total cross section was measured by the standard method of attenuating a neutron beam by a sample, which in this case was neon gas contained in a meter-long steel cylinder at high pressure. Differential cross sections were observed both by measuring neon recoil energies in a proportional counter and also by detecting neutrons with an anthracene crystal in coincidence with neon recoils. The combination of techniques shows up resonances at the following energies (in Mev) with spin and parity assignments given in parentheses: 0.91 ($\frac{3}{2}-$); 1.28 ($\frac{3}{2}-$); 1.31 ($\frac{1}{2}-$); 1.37 ($\frac{3}{2}$ or $\frac{5}{2}+$); 1.62 ($\frac{3}{2}-$); 1.68 ($\frac{3}{2}+$); and 1.85 ($\cdots$). These resonances have reduced widths of the order of one percent of the Wigner limits.

INTRODUCTION

ELASTIC scattering of neutrons from zero-spin nuclei is of special interest. Since, in such cases as the scattering of neutrons from He^4,[1–3] C^{12},[4–11] O^{16},[12–15] and Ne^{20},[16–18] there is only one channel spin state, a unique phase-shift analysis of differential scattering data is possible, at least at low energies. Phase shifts so obtained in the case of He^4 neutron scattering,[3] and also in the case of O^{16},[14] can be discussed in terms of a single-particle picture, for in these cases one is dealing with the interaction of a neutron with closed-shell nuclei. This type of analysis seems to hold approximately even for neutron scattering from C^{12}.[11] It is of some interest, then, to investigate neutron scattering from Ne^{20} which is a nucleus rather far removed from a closed shell. Such an investigation, of course, leads to detailed knowledge of virtual states of Ne^{21}. Furthermore, a phase-shift analysis of neutron scattering from light zero-spin nuclei furnishes one a tool to measure the polarization of neutron sources.[4–6,11,15,19–23]

[1] P. Huber and E. Baldinger, Helv. Phys. Acta **25**, 435 (1952).
[2] J. D. Seagrave, Phys. Rev. **92**, 1222 (1953).
[3] E. Van der Spuy, Nuclear Phys. **1**, 381 (1956).
[4] R. Ricamo, Nuovo cimento **10**, 1607 (1953).
[5] Meier, Scherrer, and Trumpy, Helv. Phys. Acta **27**, 577 (1954).
[6] R. Budde and P. Huber, Helv. Phys. Acta **28**, 49 (1955).
[7] Little, Leonard, Prud'Homme, and Vincent, Phys. Rev. **98**, 634 (1955).
[8] Willard, Bair, and Kington, Phys. Rev. **98**, 669 (1955).
[9] M. Walt and J. R. Beyster, Phys. Rev. **98**, 677 (1955).
[10] Muehlhause, Bloom, Wegner, and Glasoe, Phys. Rev. **103**, 720 (1956).
[11] Wills, Bair, Cohn, and Willard, Phys. Rev. **109**, 891 (1958).
[12] R. K. Adair, Phys. Rev. **92**, 1491 (1953).
[13] A. Okazaki, Phys. Rev. **99**, 55 (1955).
[14] J. L. Fowler and H. O. Cohn, Phys. Rev. **109**, 89 (1958).
[15] Striebel, Darden, and Haeberli, Nuclear Phys. **6**, 188 (1958).
[16] H. O. Cohn and J. L. Fowler, Phys. Rev. **99**, 1625 (1955).
[17] H. O. Cohn and J. L. Fowler, Bull. Am. Phys. Soc. Ser. II, **1**, 175 (1956).
[18] C. P. Sikkema, Nuclear Phys. **3**, 375 (1957).
[19] E. Baumgartner and P. Huber, Helv. Phys. Acta **26**, 545 (1953).
[20] Adair, Darden, and Fields, Phys. Rev. **96**, 503 (1954).
[21] Willard, Bair, and Kington, Phys. Rev. **95**, 1359 (1954).
[22] Levintov, Miller, and Shamshev, Nuclear Phys. **3**, 221 (1957).
[23] Levintov, Miller, Tarumov, and Shamshev, Nuclear Phys. **3**, 237 (1957).

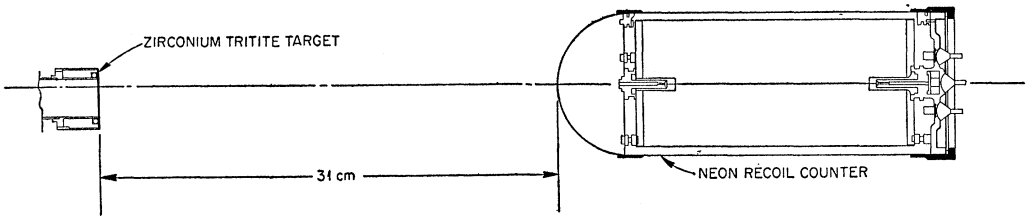

FIG. 1. Experimental arrangement for the neon recoil energy distribution measurements.

NEON RECOILS

For a preliminary study of the scattering of neutrons from neon, the technique of pulse-height analysis of nuclear recoils in a proportional counter was used for the neutron energy region 0.8 to 1.7 Mev.[16] Neutrons were produced by bombarding a rotating zirconium tritiated target with analyzed protons from the 5.5-Mv electrostatic generator.[24]

The neutron energy resolution at 1-Mev neutron energy was approximately 10 kev as determined by the rise at threshold of the yield from the tritium target. The proportional counter, which has been described elsewhere in connection with its use in analyzing nitrogen recoils,[25] is illustrated in Fig. 1 as it was aligned for this experiment. It was filled to 2 atmospheres with purified neon gas of natural abundance to which was added 2% CO_2. Neutrons were monitored with a long counter at about 120° to the forward neutron direction.

With low bias settings, the integral counts (Fig. 2, right-hand side) show up prominent resonances at neutron energies 0.91, 1.31, 1.38, 1.62, and 1.68 Mev. Subsequent measurements to be described further on in this article have shown the level at 1.31 Mev to be distorted by the presence of a resonance at 1.28 Mev, and the position of the third level is nearer 1.37 Mev.

Some of the nuclear-recoil energy spectra found by analyzing the amplified recoil pulses from the proportional counter with a 20-channel pulse-height analyzer are shown on the left-hand side of Fig. 2. The arrows indicate the energy at which the spectrum was measured. In the absence of inelastic scattering, the angular distribution of elastic scattering of neutrons can be deduced from the energy distribution of recoil nuclei.[26,27] The energy of the recoil nucleus is proportional to $1-\cos\phi$, where ϕ is the neutron scattering angle in the center-of-mass system. In this system the number of recoils in the energy interval ΔE is proportional to the differential scattering cross section times the interval $\Delta(\cos\phi)$. In Fig. 2, the upper edge of the recoil-energy distribution has been adjusted to correspond to $\cos\phi=-1$ and the pulse-height scale is labelled also as $\cos\phi$. The lower energy portion of the recoil energy spectrum is very distorted; however, an approximate interpretation can be made for the large angle neutron scattering $\phi>90°$. From these data, one concludes that the 1.37- and the 1.68-Mev levels are characterized by large backscattering of neutrons. As will be seen later, these levels correspond to d-wave neutron scattering. The other levels turn out to be due to p-wave scattering. Recently, at somewhat higher energies, >1.9 Mev, Sikkema[18] has made the neon-recoil techniques reliable by introducing an anti-coincidence ring in the proportional counter which enables one to remove much of the background due to gamma rays. In the case of low-energy neon recoils, another technique described in a following section allows one to greatly improve the quality of the data.

NEON TOTAL CROSS SECTION

The absolute total neutron cross section of neon was measured for neutron energies from 0.8 to 1.9 Mev by a transmission experiment.[28] $Li^7(p,n)Be^7$ neutrons were

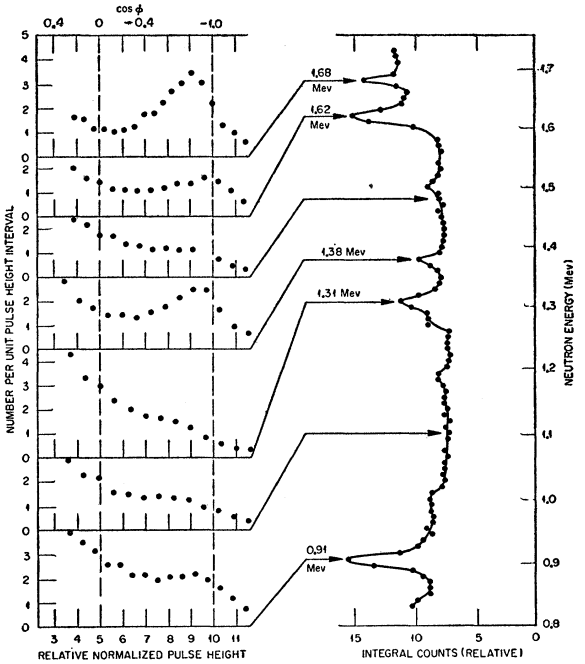

FIG. 2. Results of the neon recoil experiment. The left-hand graphs give the pulse-height distribution observed for neon recoils at neutron energies indicated by the arrows. The right-hand curve shows the integral of the neon recoil curves as a function of neutron energy.

[24] Kington, Bair, Cohn, and Willard, Phys. Rev. **99**, 1393 (1955).
[25] J. L. Fowler and C. H. Johnson, Phys. Rev. **98**, 728 (1955).
[26] Baldinger, Huber, and Staub, Helv. Phys. Acta **11**, 245 (1938).
[27] H. H. Barschall and M. H. Kanner, Phys. Rev. **58**, 590 (1940).
[28] H. O. Cohn and J. L. Fowler, Bull. Am. Phys. Soc. Ser. II, **3**, 18 (1958).

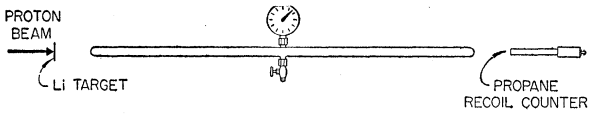

FIG. 3. Experimental arrangement for total cross-section measurement.

produced at a rotating Li target with protons from the ORNL-5.5-Mv Van de Graaff. The detector was a 1-atmosphere propane recoil counter. A 39 in. long and $\frac{7}{8}$ in. (i.d.) thin-walled ($\frac{1}{16}$ in.) stainless steel tube, shown in Fig. 3, filled to 1200 lb/in.^{2} with natural neon gas served as the scattering sample. The tube was filled by first freezing neon gas in a container of small volume immersed in liquid helium, and then allowing the gas to expand into the sample tube. Spectroscopic analysis of neon taken from the sample tube showed it to contain no more than 0.09% impurities. A similar tube, but evacuated, was used to correct experimentally for the effects due to the stainless steel.

The total cross-section curve, shown in Fig. 4, was obtained with neutrons of about 13-kev energy resolution. The errors shown arise from statistics. The uncertainty in the neutron energy scale was less than 5 kev.[24] The points have been corrected for the second group of neutrons from the $Li^7(p,n)Be^7$ reaction, as well as for a small background as measured with a Lucite shadow cone. In-scattering corrections were less than $\frac{1}{2}$% and were neglected. All resonances that were obtained from the recoil counter experiment by integrating the differential cross section (Fig. 2) were observed as well as a resonance at 1.85 Mev not covered by the other method.

Fluctuations of some of the points on the total cross-section curve were due to small resonances also observed by the integrated differential cross-section measurements. Because neon of natural isotopic abundance was used, however, such resonances could be due to the ~10% abundant isotope Ne^{22}, and were ignored in this analysis.

Neutron energies for which resonances were observed in Ne^{20} are: E_n=0.91, 1.28, 1.31, 1.37, 1.62, 1.68, and 1.85 Mev. Three additional analyzed resonances at neutron energies not covered by this experiment were reported by Sikkema[18] at E_n=1.94 and 2.00 Mev, and by Walt[29] at about 0.5 Mev.

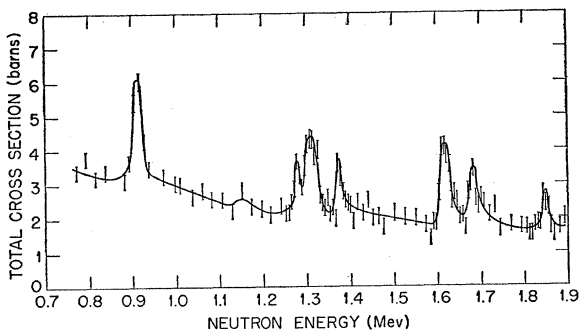

FIG. 4. Total cross section of neon.

The energies of the resonances as well as their spin and parity assignments (to be discussed later on) from the present work, as well as from Sikkema's and Walt's measurements, are summarized in Table I.

NEUTRON-NEON RECOIL COINCIDENCES

Because of the difficulty of interpretation of the neon recoil information given in Fig. 2, a method was devised for measuring more directly the differential elastic scattering cross section for nuclei in a gaseous form.[17] Figure 5 shows the experimental apparatus. Here again the neutron source is the $T(p,n)$ reaction produced by protons bombarding a zirconium tritiated target. The LiF-impregnated paraffin shield has a rectangular slot to allow source neutrons to be incident upon the 2-in. diameter, 5-in. long counting volume of the proportional counter adapted from the neon recoil experiment shown in Fig. 1. Real coincidences were observed between proton recoils in the anthracene crystal and

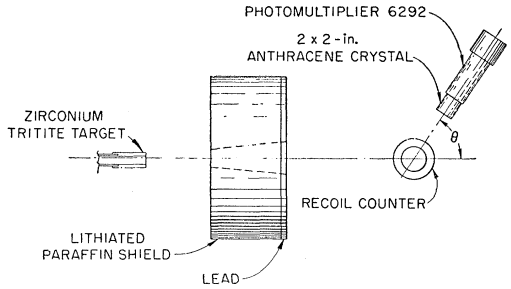

FIG. 5. Experimental arrangement for measuring the differential cross section of neon gas. The construction of the proportional counter is shown in Fig. 1.

neon recoils in the proportional counter. A typical proton recoil spectrum in the anthracene crystal is given in Fig. 6. In this case the primary neutron energy was 1.56 Mev. The window of a single-channel analyzer was adjusted to accept pulses between the limits indicated in Fig. 6, and the output was gated in a coincidence circuit. The pulse from the integral bias discriminator of the neon-counter amplifier furnished a gate for the other channel of the coincidence circuit. In order to improve the ion collection time in the Ne counter, 2% CO_2 was added to the neon gas.

In setting up the experiment, the coincidence rate was measured as a function of the delay of one channel relative to the other. The curve obtained indicated that the width of the coincidence gate was adequate for the collection time of the neon counter. With a sufficiently long delay (4.7 μsec) in one channel, the accidental resolving time which was controlled by the coincidence gate was found to be about 2.6 μsec. This resolving time measurement was repeated periodically

[29] M. Walt (private communication); Vaughn, Imhof, Johnson, and Walt, Bull. Am. Phys. Soc. Ser. II, 3, 165 (1958).

TABLE I. Resonance parameters of neon, and potential phase shifts used in fitting data.

E_0 Mev	Γ kev	J	l	π	Percent of Wigner limit	Potential scattering phase shifts[a] $\delta_{s1/2}$	$\delta_{p1/2}$	$\delta_{p3/2}$	References
0.5	...	$\frac{1}{2}$	0	+	...	...	...	...	b
0.91	14±30%	$\frac{3}{2}$	1	−	0.6	−73°	0	0	Present work
1.28	6±30%	$\frac{3}{2}$	1	−	0.2	−78°	−7°	−8°	Present work
1.31	32±20%	$\frac{1}{2}$	1	−	1.1	−78°	−7°	−9°	Present work
1.37	9(5)[c]±30%	$\frac{3}{2}$ ($\frac{5}{2}$)	2	+	1.0 (0.6)	−79°	−8°	−9°	Present work
1.62	27±20%	$\frac{3}{2}$	1	−	0.8	−80°	−9°	−11°	Present work
1.68	10±30%	$\frac{3}{2}$	2	+	0.8	−80°	−10°	−11°	Present work
1.85	...	...	...	...	...	...	...	...	Present work
1.94[e]	20±50%	$\frac{3}{2}$	2	+	1.3	...	...	...	d
2.00[e]	50±20%	$\frac{3}{2}$	1	−	1.3	...	...	...	d

[a] Potential scattering phase shifts used to calculate the angular distributions shown in Figs. 7, 8, and 9.
[b] See reference 29.
[c] Assignment indefinite; quantities in parentheses go together.
[d] See reference 18.
[e] *Note added in proof.*—Dr. C. P. Sikkema informs us that more recent measurements give the widths of the 1.94 and 2.00 Mev levels to be, respectively, 32±10 kev and 48±10 kev.

throughout the experiment. The beam current was adjusted during most of the subsequent runs to give an accidental rate the order of one-half the real coincidence rate. Bias curves for the neon recoil counter were obtained by measuring the coincidence rate as a function of the integral bias of the neon amplifier. For each angular setting for the differential cross section measurements, the integral bias was set well on the plateaus of these bias curves.

Absolute differential cross sections were obtained from the coincidence data by measuring the direct neutron flux with the neutron detecting crystal, rotated into the direct beam. For calculating the absolute cross section, the relative efficiency of the neutron detector is needed as a function of energy over the range of neutron recoil energies as well as knowledge of the geometry of the experiment and the number of neon nuclei in the active volume of the neon counter. As in the case of scattering from solid samples, the relative efficiency of the crystal as a function of neutron energy was determined by comparing the response of the biased crystal with a long counter,[8,25] both of which were at 5° to the forward neutron direction of the T(p,n) source.

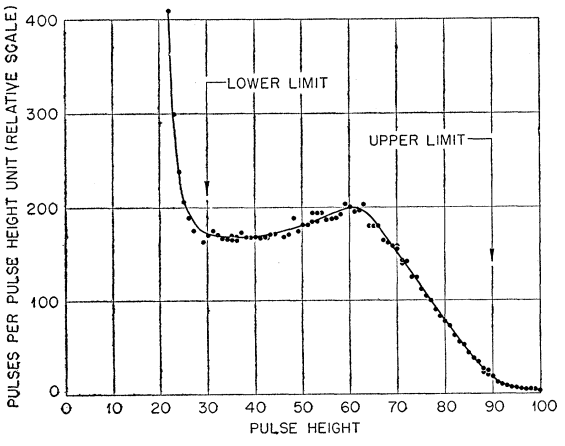

FIG. 6. Distribution of pulses in the anthracene crystal resulting from 1.56-Mev neutrons. Bias limits are indicated by arrows.

Background other than that due to accidental coincidences was evaluated by removing the direct neutrons with a 7-in. thick LiF-impregnated plug inserted in the slot in the shielding. This type of background, presumably arising from γ rays producing real coincidences by Compton scattering, amounted to about 30%. It was measured periodically during the course of the experiment at each of the several angular settings of the crystal. At the neutron energies below 1.43 Mev, the absolute cross-section measurements corrected for background as described above, agreed rather well with that expected from the total cross-section curve of Fig. 4. (See Figs. 7 and 8.) Between 1.57 and 1.76 Mev, however, there appeared to be an additional source of background. The fit of the data, both for the resonances as well as for the positions

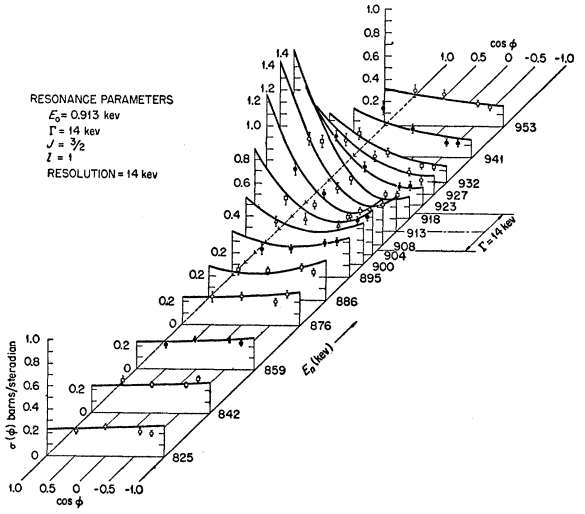

FIG. 7. Center-of-mass differential cross sections of neon in the vicinity of the 0.91-Mev level. Energy is laboratory energy of neutron. The solid curves are calculated from the set of parameters indicated in figure, and with the potential phase shifts listed in Table I.

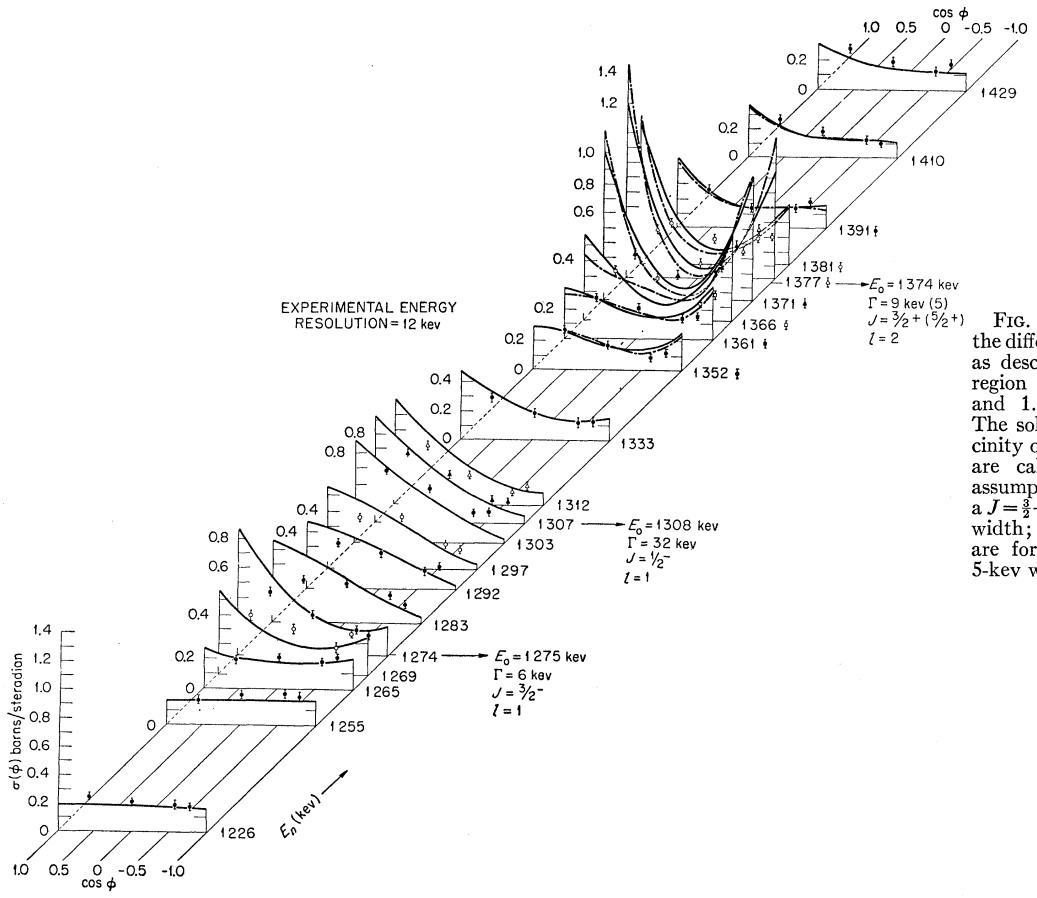

FIG. 8. An extension of the differential cross sections as described in Fig. 7 into region of the 1.28-, 1.31-, and 1.37-Mev resonances. The solid curves in the vicinity of the 1.37-Mev level are calculated under the assumption that this level is a $J=\frac{3}{2}+$ resonance of 9-kev width; the dashed curves are for a $J=\frac{5}{2}+$ level of 5-kev width.

between the resonances, to the theoretical curves of Fig. 9 which give the measured total cross section was obtained only after a constant background of ~100 millibarns was subtracted from the original differential data. Part of this background could arise from neutrons being inelastically scattered from the steel in the neon counter, and from the lead in the vicinity of the slot through the shield, in which case the inelastically scattered neutron could give a neon recoil which is in coincidence with the inelastic γ ray detected by the organic crystal. Or γ rays produced along with neutrons at the source could Compton-scatter an electron in the neon counter and be detected in coincidence in the organic crystal. Real coincidences due to either of these causes should be expected to decrease rapidly with decreasing energy. The detection efficiency for the inelastically scattered neutrons falls off rapidly with decreasing energy as well as the inelastic scattering cross section itself, and the number of γ rays from the source should decrease considerably with decreasing proton energy. In any case, there seemed to be no appreciable background present in the case of the differential curves at lower energies (Figs. 7 and 8).

RESULTS AND CONCLUSIONS

For resolved resonances, measurements of the neutron total cross section allow an assignment of the total angular momentum associated with the resonance. The value of the cross section at resonance is given by

$$4\pi\lambda\!\!\!^{-2}[(2J+1)/(2I+1)(2s+1)](\Gamma_n/\Gamma)^2,$$

where J is the total angular momentum quantum number, I and s are the spin of the target and neutron, respectively, $\lambda\!\!\!^{-}$ is the neutron wavelength divided by 2π, and Γ_n/Γ is the ratio of the neutron resonance width to the total width. For the system $Ne^{20}+n$ in the energy range 0.8 to 1.9 Mev, the only effective competition for neutron emission is α emission, which is observed to be very small.[30] Thus the total cross section presented in Fig. 4, corrected for the energy resolution of the neutron source (13 kev), identifies the three broad resonances as $J=\frac{3}{2}$ at 0.91 Mev, $J=\frac{1}{2}$ at 1.31 Mev, and $J=\frac{3}{2}$ at 1.62 Mev. With less certainty because of the larger correction for energy resolution, the level at 1.68 Mev is assigned a J value of $\frac{3}{2}$. Additional information is necessary to give the parity of these

[30] Johnson, Bockelman, and Barschall, Phys. Rev. **82**, 117 (1951).

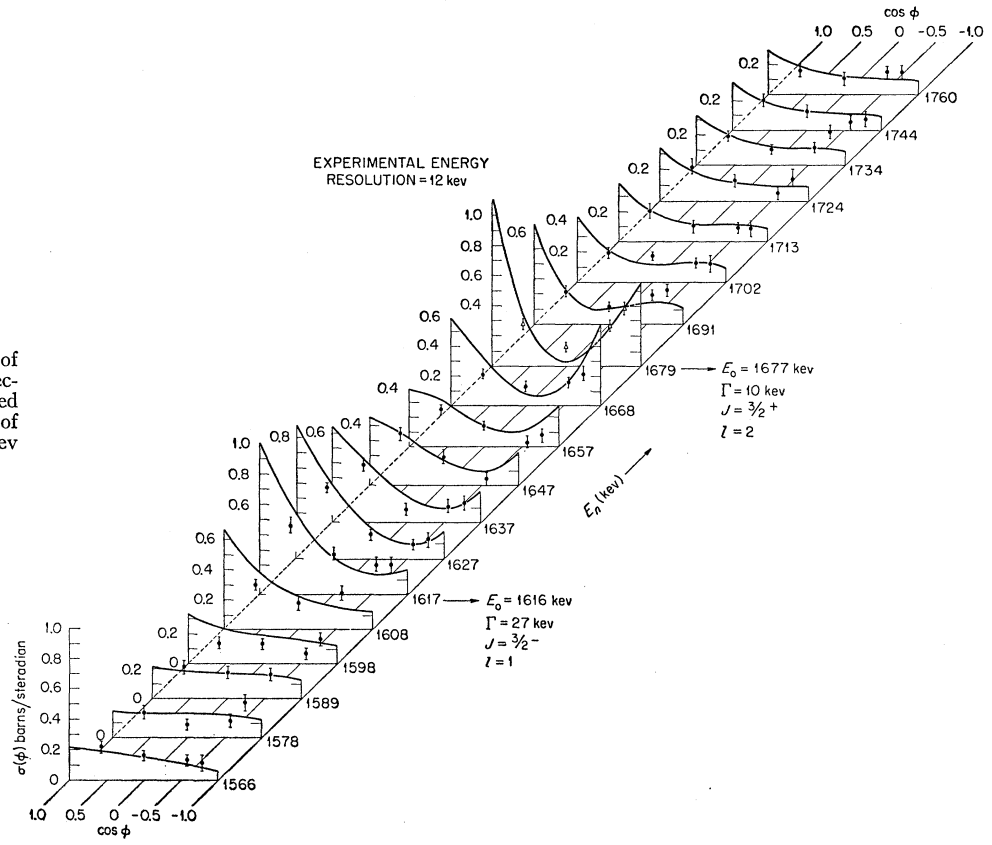

FIG. 9. An extension of the differential cross sections of neon, as described in Fig. 7, into the region of the 1.62- and 1.68-Mev levels.

levels and to assign the quantum numbers to the other levels.

Such additional information is available from the differential scattering cross section measurements obtained from the coincidence experiment described in the previous section. The results are plotted in Figs. 7, 8, and 9. The vertical scales of the figures give the cross sections in barns per steradian in the center-of-mass system. The horizontal scales give the cosine of the center-of-mass angle. Neutron energy in the laboratory system is given on the skew scales. Errors shown are due to statistics. The solid lines are calculated by use of the Breit-Wigner resonance formalism.[31,5] Resonance width variation with energy and the effect of the experimental energy and angular resolution are included in the theoretical curves as well as an estimate of the effects of isotopes in the recoil counter (Ne^{21}, Ne^{22}, C, and O) other than Ne^{20}. The assumption was made that the scattering due to these isotopes, except in the case of oxygen, was the same as the nonresonant scattering of Ne^{20}. For oxygen in the vicinity of the 1-Mev resonance, the measured differential cross section[14] was used in making the correction. In calculating the resonance width variation with energy as well as the reduced widths estimated for Table I, the radius of interaction for Ne was taken as $R=1.4(A^{\frac{1}{3}}+1)\times10^{-13}$ cm.

In the vicinity of 0.91 Mev, the differential measurements (Fig. 7) are fit rather well under the assumption that the $J=\frac{3}{2}$ level of width 14 kev is due to p-wave neutrons interfering with s-wave potential scattering. An s-wave phase shift of about $-73°$ at 0.91 Mev and its variation with energy was assumed in order to fit the total cross section shown in Fig. 4 (Table I).

For the next energy region, Fig. 8, three resonances are involved. Only one can be assigned a J value from the total cross section alone. Since this level at 1.31 Mev has $J=\frac{1}{2}$, it can only be a s or p resonance. The lack of interference with s-wave potential scattering in the total cross section indicates a p-wave level, and the differential measurements of Fig. 8 confirm this assignment. Asymmetry about $\cos\phi=0$ in the center-of-mass system indicates the 1.28-Mev resonance is also a p-wave level, and hence has $J=\frac{1}{2}$ or $\frac{3}{2}$. The observed width of this level, which is only slightly more than the experimental resolution of 13 kev, shows that the level is very narrow, probably under 8 kev wide. For such a narrow level, the height of the resonance observed under an energy resolution of 13 kev, if $J=\frac{1}{2}$, would be less than 0.9 barn. The total cross-section data in Fig. 4 favors a $J=\frac{3}{2}$ assignment for this

[31] J. M. Blatt and L. C. Biedenharn, Revs. Modern Phys. **24**, 258 (1952).

1.28-Mev level. Furthermore, two levels having the same angular momentum and parity cannot overlap in the manner in which the 1.28 and the 1.31-Mev level appear to overlap in Fig. 4. The differential cross-section data in Fig. 8 are consistent with the assignment of $J=\frac{3}{2}$, $l=1$, $\Gamma=6$ kev for the 1.28-Mev level, and $J=\frac{1}{2}$ $l=1$, $\Gamma=32$ kev for the 1.31-Mev level. In addition to a s-wave potential scattering phase shift of about $-78°$ at 1.31 Mev, p-wave potential phase shifts both for the $p^{\frac{3}{2}}$ state as well as the $p^{\frac{1}{2}}$ state were assumed in order to fit the total cross section and the nonresonant differential scattering data shown in Fig. 8. $p^{\frac{1}{2}}$ potential phase shifts were taken slightly larger in absolute magnitude in order to allow for the tail of the lower energy, $J=\frac{3}{2}$ resonance (Table I).

For the 1.37-Mev level, the nonisotropic but approximate symmetric differential cross section about $\cos\phi=0$ (Fig. 8), indicates a $J>\frac{1}{2}$ even parity level, almost certainly a d level. From the value of the total cross section, Fig. 4, the resonance is either a 9 kev $J=\frac{3}{2}$ level or a somewhat narrower (5 kev) $J=\frac{5}{2}$ level. The expected differential cross sections for the $J=\frac{3}{2}$, $l=2$, $\Gamma=9$ kev are shown as solid lines in Fig. 8 from 1.35 to 1.41 Mev. Dashed lines are for the $J=\frac{5}{2}$, $l=2$, $\Gamma=5$-kev assignment. Even the angular distribution data does not differentiate between these two cases, although the $J=\frac{3}{2}+$, $\Gamma=9$ kev assignment seems slightly favored by the data.

In the last energy range covered by the differential cross section measurements, 1.56 to 1.75 Mev, two resonances are observed. The one at 1.62 Mev has a width sufficiently large that its J value$=\frac{3}{2}$ can be obtained from the total cross section. The angular distribution is that due to p-wave scattering so that the resonance is identified as a $J=\frac{3}{2}$, $l=1$, $\Gamma=27$-kev level. Theoretical curves calculated for such a resonance are in agreement with the experimental differential data (Fig. 9). The angular distribution information at the 1.68-Mev resonance indicates an even parity level with $J>\frac{1}{2}$, that is, a d level, so that the possibilities are $J=\frac{5}{2}+$ or $J=\frac{3}{2}+$. The observed width in the total cross section is consistent for a $\Gamma=10$-kev level. A $J=\frac{3}{2}$ level of this width observed with 13-kev energy resolution would have a resonance peak total cross section of 1.6 barns; a $J=\frac{5}{2}$ level would have 2.4 barns. The observed resonance peak cross section of 1.7 ± 0.4 barns definitely favors the $J=\frac{3}{2}$ assignment. The calculated curves for a $J=\frac{3}{2}$, $l=2$, $\Gamma=10$-kev level at 1.68 Mev agree with this assignment. For the range of energies covered in Fig. 9, the s-wave potential phase shifts are taken to be about $-80°$; the p-wave potential phase shifts about $-10°$ (Table I).

Table I summarizes the results of this analysis as well as other information available in the literature on scattering of neutrons from Ne^{20}. It is of interest to examine this information in the light of what is known about neutron scattering from other light nuclei. In the case of He^4 and O^{16}, and to a less extent in the case of C^{12}, there are states observed by neutron elastic scattering which have large, almost single-particle reduced widths. This is particularly true for the odd-parity states of He^5 [3] and the even-parity states of O^{17} and C^{13}.[14] For Ne^{21}, the maximum reduced width is only of the order of 1% of the Wigner limit (Table I). In Ne^{21}, one is filling the $1d$ and $2s$ shells far from a closed shell. There is as a consequence a great deal of configuration mixing, and hence one observes a relatively large number of reasonably narrow resonances.

ACKNOWLEDGMENTS

We wish to acknowledge the assistance of Dr. J. W. T. Dabbs of this Laboratory in preparing the neon sample for the total cross section measurements. We are indebted to Mr. W. T. Newton and Mr. A. J. Wyrick for aid in taking data. We also thank Mr. D. O. Patterson and Mr. C. E. Hughey, Cooperative Engineering Students from the University of Tennessee, for much of the detailed computations which were necessary for fitting the resonance parameters to the data.